PRAMANA — journal of physics

Vol. 78, No. 5
May 2012
pp. 737–748

Nucleon momentum distributions and elastic electron scattering form factors for some 1p-shell nuclei

A K HAMOUDI, M A HASAN* and A R RIDHA
Department of Physics, College of Science, University of Baghdad, Baghdad, Iraq
*Corresponding author. E-mail: marwan.a.hasan@gmail.com

MS received 28 May 2011; revised 14 September 2011; accepted 23 December 2011

Abstract. The nucleon momentum distributions (NMD) and elastic electron scattering form factors of the ground state for 1p-shell nuclei with $Z = N$ (such as ^{6}Li, ^{10}B, ^{12}C and ^{14}N nuclei) have been calculated in the framework of the coherent density fluctuation model (CDFM) and expressed in terms of the weight function $|f(x)|^2$. The weight function has been expressed in terms of nucleon density distribution (NDD) of the nuclei and determined from the theory and the experiment. The feature of the long-tail behaviour at high-momentum region of the NMDs has been obtained by both the theoretical and experimental weight functions. The experimental form factors $F(q)$ of all the considered nuclei are very well reproduced by the present calculations for all values of momentum transfer q. It is found that the contributions of the quadrupole form factors $F_{C2}(q)$ in ^{10}B and ^{14}N nuclei, which are described by the undeformed p-shell model, are essential for obtaining a remarkable agreement between the theoretical and experimental form factors.

Keywords. Mean square radii; nucleon density distributions; nucleon momentum distributions; elastic electron scattering form factors.

PACS No. 25.30.Bf

1. Introduction

High-energy elastic electron scattering is a clear and precise tool for probing nuclear structure, particularly, cross-sections, form factors and nucleon densities [1,2]. Half a century ago, Hofstadter *et al* [3,4] have done the pioneering study of electron scattering on atomic nuclei. Since then, a lot of work has been done in this area, and many valuable and precise data on the nuclear electromagnetic properties have been accumulated [5,6]. Electrons interact with nuclei basically through the electromagnetic force. If the energy of the electrons is high enough, they become a relatively clean probe to explore precisely the internal structure of the nuclei [7]. There are many reasons why inclusive electron scattering provides a powerful tool for studying the structure of nuclei

and nucleons. First, the interaction is known and second, the interaction is relatively weak, thus one can make measurements without greatly disturbing the structure of the target [8]. Several theoretical methods, such as the plane-wave Born approximation (PWBA), the eikonal approximation and the phase-shift analysis method are used to study elastic electron–nucleus scattering. The PWBA method can give qualitative results and has been used widely because of its simplicity. To include the Coulomb distortion effect, which is neglected in PWBA, the other two methods may be used [9]. For light nuclei where $Z\alpha \ll 1$ (α is the fine-structure constant), one can use, to a good approximation, the PWBA to describe the scattering process [10]. In the PWBA, the incident and scattered electron waves are considered as plane waves. The elastic electron scattering form factors from spin zero nuclei can be determined purely by the ground state density distribution, where the form factor is the Fourier transform of the density distribution and vice versa [11]. In the past few years, some theoretical studies of elastic and inelastic electron scattering form factors of 1p-shell nuclei have been performed [12–17].

No method is available for directly measuring NMD in nuclei. The quantities that are measured by particle–nucleus and nucleus–nucleus collisions are the cross-sections of different reactions, and these contain information on the NMD of target nucleons. The experimental evidence obtained from inclusive and exclusive electron scattering on nuclei established the existence of long-tail behaviour of NMD at high momentum region ($k \geq 2$ fm^{-1}) [18–21]. In principle, the mean-field theories cannot correctly describe NMD and form factors $F(q)$ simultaneously [22] and they exhibit a steep-slope behaviour of NMD at high-momentum region. In fact, NMD depends a little on the effective mean-field considered due to its sensitivity to short range and tensor nucleon–nucleon correlations [22,23] which are not included in the mean-field theories.

In coherent density fluctuations model (CDFM), which is exemplified by the work of Antonov *et al* [18,24,25], the local density distribution and NMD are simply related and expressed in terms of experimentally obtainable fluctuation function (weight function) $|f(x)|^2$. They [18,24,25] studied the NMD of (^{4}He and ^{16}O), ^{12}C and (^{39}K, ^{40}Ca and ^{48}Ca) nuclei using weight functions $|f(x)|^2$ expressed in terms of, respectively, the experimental NDD of 2PF, the experimental NDD of 3PF and the experimental NDD model-independent Fourier–Bessel analysis or sum of Gaussians [26,27]. It is important to point out that all these calculations obtained in the framework of CDFM proved a high momentum tail in the NMD. Elastic electron scattering from ^{40}Ca nucleus was also investigated in [18], where the calculated elastic differential cross-sections $\mathrm{d}\sigma/\mathrm{d}\Omega$ are in good agreement with the experimental data.

The aim of the present study is to derive an analytical form for the NDD, applicable throughout all p-shell nuclei, based on the single particle harmonic oscillator wave functions and the occupation numbers of the states. The derived form of the NDD is employed to determine the theoretical weight function $|f(x)|^2$ which is used in the CDFM to study the NMD and elastic $F(q)$ for some 1p-shell nuclei with $Z = N$, such as, ^{6}Li, ^{10}B, ^{12}C and ^{14}N nuclei. We shall see later that the theoretical $|f(x)|^2$, based on the derived form of the NDD, is capable to give information about the NMD and elastic $F(q)$ as do those of the experimental two-parameter Fermi (2PF), three-parameter Fermi (3PF) and harmonic oscillator (HO) densities [26].

2. Theory

The nucleon density distribution (NDD) of the one-body operator can be written as [28,29]

$$\rho(r) = \frac{1}{4\pi} \sum_{nl} \eta_{nl} 4(2l+1) \left|R_{nl}(r)\right|^2, \tag{1}$$

where η_{nl} is the nucleon occupation probability of the state nl ($\eta_{nl} = 0$ or 1 for closed shell nuclei and $0 < \eta_{nl} < 1$ for open shell nuclei) and $R_{nl}(r)$ is the radial part of the single-particle harmonic oscillator wave function. To derive an explicit form for the NDD of 1p-shell nuclei, we assume that there is a core of filled 1s shell and the nucleon occupation numbers in 1p, $2s_{1/2}$ and $1f_{7/2}$ orbitals are equal to, respectively, $(A-4-\alpha)$, α_1 and α_2, and not to $(A-4)$, 0 and 0 as in the simple shell model. Using this assumption in eq. (1), an analytical form for the ground state NDD of the 1p-shell nuclei is obtained as

$$\rho(r) = \frac{2}{\pi^{3/2} b^3} \exp\left(\frac{-r^2}{b^2}\right) \times \left[2 + \frac{3\alpha_1}{4} + \frac{(A-4-\alpha-3\alpha_1)}{3}\left(\frac{r}{b}\right)^2 + \frac{\alpha_1}{3}\left(\frac{r}{b}\right)^4 + \frac{4\alpha_2}{105}\left(\frac{r}{b}\right)^6\right], \tag{2}$$

where A is the nuclear mass number, b is the size parameter of the harmonic oscillator and α ($4 = \alpha_1 + \alpha_2$) is the deviation of the nucleon occupation numbers from the predicted value of the simple shell model ($\alpha = 0$). It is important to remark that for $Z = N$ nuclei (Z and N are the proton and neutron numbers), the ground state charge density distribution CDD, $\rho_{\mathrm{ch}}(r)$, is related to the ground state NDD by $\rho_{\mathrm{ch}}(r) = \rho(r)/2$ [31].

The normalization condition of the NDD is given by [18,26]

$$A = 4\pi \int_0^\infty \rho(r) r^2 \, \mathrm{d}r \tag{3}$$

and the mean square radius (MSR) of the considered 1p-shell nuclei is given by [18,26]

$$\langle r^2 \rangle = \frac{4\pi}{A} \int_0^\infty \rho(r) r^4 \, \mathrm{d}r. \tag{4}$$

The central NDD, $\rho(r = 0)$, is obtained from eq. (2) as

$$\rho(0) = \frac{2}{\pi^{3/2} b^3}\left[2 + \frac{3\alpha_1}{4}\right]. \tag{5}$$

Then α_1 is obtained from eq. (5) as

$$\alpha_1 = \frac{2(\rho_0(0)\pi^{3/2} b^3 - 4)}{3}. \tag{6}$$

Substituting eq. (2) into eq. (4) and after simplification we get

$$\langle r^2 \rangle = \frac{b^2}{A}\left[\frac{5}{2}A - 4 - \alpha_1 + 2\alpha\right]. \tag{7}$$

The parameter α is obtained by substituting eq. (6) into eq. (7) as

$$\alpha = \frac{A}{2b^2}\langle r^2\rangle + 2 - \frac{5}{4}A + \frac{1}{3}(\rho(0)\pi^{3/2}b^3 - 4). \tag{8}$$

The parameter α_2 is then obtained using the equation $\alpha_2 = \alpha - \alpha_1$. In eqs (6) and (8), the values of $\rho(0)$ and $\langle r^2\rangle$ are taken from the experiments while the parameter b is chosen in such a way as to reproduce the experimental root mean square radii of the nuclei.

The nucleon momentum distribution, $n(k)$, for the 1p-shell nuclei is studied using two distinct methods. In the first method, it is determined by the shell model using the single-particle harmonic oscillator wave functions in momentum representation and is given by [30]

$$n(k) = \frac{2b^3}{\pi^{3/2}}\mathrm{e}^{-b^2k^2}\left[2 + \frac{(A-4)}{3}(bk)^2\right]. \tag{9}$$

In the second method, the NMD is determined by the CDFM, where the mixed density is given by [18,24]

$$\rho(r, r') = \int_0^\infty |f(x)|^2\, \rho_x(r, r')\mathrm{d}x \tag{10}$$

since

$$\rho_x(r, r') = 3\rho_0(x)\frac{j_1(k_\mathrm{F}(x)|\bar{r} - \bar{r}'|)}{k_\mathrm{F}(x)\,|\bar{r} - \bar{r}'|}\theta\left(\bar{x} - \frac{1}{2}|\bar{r} + \bar{r}'|\right) \tag{11}$$

is the density matrix for A-nucleons uniformly distributed in the sphere with radius x and fixed mean density $\rho_0(x)$ where

$$\rho_0(x) = \frac{3A}{4\pi x^3}. \tag{12}$$

The step function θ, in eq. (11), is defined as

$$\begin{aligned}\theta\,(y) &= 1, \quad \text{for } y \geq 0\\ &= 0, \quad \text{for } y < 0\end{aligned} \tag{13}$$

and the Fermi momentum is defined as

$$k_\mathrm{F}(x) = \left(\frac{3\pi^2}{2}\rho_0(x)\right)^{1/3} \equiv \frac{\eta}{x}, \quad \eta \equiv \left(\frac{9\pi A}{8}\right)^{1/3}. \tag{14}$$

According to the density matrix definition of eq. (10), one-particle density $\rho(r)$ is given by it's diagonal elements as

$$\rho(r) = \rho(r, r')\big|_{r=r'} = \int_0^\infty |f(x)|^2\, \rho_x(r)\mathrm{d}x. \tag{15}$$

In eq. (15), $\rho_x(r)$ and $|f(x)|^2$ have the forms [18,24]

$$\rho_x(r) = \rho_0\,(x)\,\theta\,(x - r)\,, \tag{16}$$

$$|f(x)|^2 = \frac{-1}{\rho_0(x)}\left.\frac{\mathrm{d}\rho(r)}{\mathrm{d}r}\right|_{r=x}. \tag{17}$$

It is important to point out that the weight function $|f(x)|^2$ of eq. (17), determined in terms of the ground state NDD, satisfies the normalization condition

$$\int_0^\infty |f(x)|^2 \, \mathrm{d}x = 1 \tag{18}$$

and holds only for monotonically decreasing NDD, i.e. $(\mathrm{d}\rho(r)/\mathrm{d}r) < 0$ [18,24].

On the basis of eq. (15), the NMD is expressed as [18,24]

$$n(k) = \int_0^\infty |f(x)|^2 \, n_x(k) \, \mathrm{d}x, \tag{19}$$

where

$$n_x(k) = \frac{4}{3}\pi x^3 \theta(k_\mathrm{F}(x) - |\vec{k}|) \tag{20}$$

is the Fermi-momentum distribution of a system with density $\rho_0(x)$. By means of eqs (17), (19) and (20), an explicit form for the NMD is expressed in terms of $\rho(r)$ as

$$n_{\mathrm{CDFM}}(k;[\rho]) = \left(\frac{4\pi}{3}\right)^2 \frac{4}{A}\left[6\int_0^{\eta/k} \rho(x)\, x^5 \mathrm{d}x - \left(\frac{\eta}{k}\right)^6 \rho\left(\frac{\eta}{k}\right)\right]. \tag{21}$$

The normalization condition of eqs (9) and (21) is given by [24]

$$\int n_{\mathrm{CDFM}}(k) \frac{\mathrm{d}^3k}{(2\pi)^3} = A. \tag{22}$$

The elastic monopole form factors $F_{C0}(q)$ of the target nucleus is also expressed in the CDFM as [18,24]

$$F_{C0}(q) = \frac{1}{A}\int_0^\infty |f(x)|^2 \, F(q,x)\mathrm{d}x, \tag{23}$$

where the form factor of uniform nucleon density distribution is given by [24]

$$F(q,x) = \frac{3A}{(qx)^2}\left[\frac{\sin(qx)}{(qx)} - \cos(qx)\right]. \tag{24}$$

Inclusion of the corrections of the nucleon finite size $f_{\mathrm{fs}}(q)$ and the centre of mass corrections $f_{\mathrm{cm}}(q)$ in the calculations requires multiplying the form factor of eq. (23) by these corrections. Here, $f_{\mathrm{fs}}(q)$ is considered as free nucleon form factor which is assumed to be the same for protons and neutrons. This correction takes the form [31]

$$f_{\mathrm{fs}}(q) = \mathrm{e}^{\left(\frac{-0.43q^2}{4}\right)}. \tag{25}$$

The correction $f_{\mathrm{cm}}(q)$ removes the spurious state arising from the motion of the centre of mass when shell model wave function is used and is given by [31]

$$f_{\mathrm{cm}}(q) = \mathrm{e}^{\left(\frac{b^2q^2}{4A}\right)}. \tag{26}$$

It is important to point out that all physical quantities studied in the framework of the CDFM such as the NMD and form factors are expressed in terms of the weight function

$|f(x)|^2$. In refs [18,24], the weight function was obtained from the two-parameter Fermi NDD, $\rho_{2\mathrm{PF}}(r)$, extracted by analysing elastic electron–nuclei scattering experiments. In the present study, the weight function $|f(x)|^2$ is obtained from theoretical consideration, using the derived NDD of eq. (2) in eq. (17), and is given by

$$|f(x)|^2 = \frac{8\pi x^4}{3Ab^2}\rho(x) - \frac{16x^4 \mathrm{e}^{-x^2/b^2}}{3A\sqrt{\pi}b^5} \times \left[\frac{(A-4-\alpha-3\alpha_1)}{3} + \frac{2\alpha_1}{3}\left(\frac{x}{b}\right)^2 + \frac{4(\alpha-\alpha_1)}{35}\left(\frac{x}{b}\right)^4\right]. \quad (27)$$

In this study, the quadrupole form factors, which are important in ^{10}B and ^{14}N nuclei, are described by the undeformed p-shell model as [32]

$$F_{C2}(q) = \frac{\langle r^2\rangle}{Q}\left(\frac{4}{5P_J}\right)^{1/2}\int j_2(qr)\rho_{2\mathrm{ch}}(r)r^2\mathrm{d}r, \quad (28)$$

where $j_2(qr)$ is the spherical Bessel functions, Q is the quadrupole moment which is considered as a free parameter to fit the theoretical form factors with the experimental data, $\rho_{2\mathrm{ch}}(r)$ is the quadrupole charge density distributions. According to the undeformed p-shell model, we assume that the dependence of the quadrupole charge density distributions $\rho_{2\mathrm{ch}}(r)$ is the same as that of the ground state charge density distributions $\rho_{\mathrm{ch}}(r)$ and P_J is a quadrupole projection factor given by $P_J = J(2J-1)/(J+1)(2J+3)$, where J is the ground state angular momentum (J = 3 and 1 for ^{10}B and ^{14}N, respectively).

3. Results and discussion

The nucleon momentum distribution and elastic electron scattering form factors for some 1p-shell nuclei are carried out using the CDFM. The distribution of eq. (21) is calculated by means of the NDD obtained firstly from theoretical consideration as in eq. (2) and secondly from experiments, such as, 2PF, 3PF and HO [26]. The harmonic oscillator size parameters b are chosen in such a way as to reproduce the experimental root mean square radii (rms) of the nuclei. The parameters α_1 and α are determined by eqs (6) and (8), respectively. Then the parameter α_2 is determined using the equation $\alpha_2 = \alpha - \alpha_1$. In table 1, we present the values of the parameters b, α, α_1, α_2 and Q together with the experimental values of c, a, z, t, $\rho_{\mathrm{exp}}(0)$ and $\langle r^2\rangle^{1\,2}_{\mathrm{exp}}$ employed in the present calculations for ^{6}Li, ^{10}B, ^{12}C and ^{14}N nuclei.

The dependence of the NDD (in fm^{-3}) on r (in fm) for ^{6}Li, ^{10}B, ^{12}C and ^{14}N nuclei are displayed in figure 1. The long-dashed and solid curves represent the calculated NDD, using eq. (2), with $\alpha = \alpha_1 = \alpha_2 = 0$ and $\alpha \neq \alpha_1 \neq \alpha_2 \neq 0$, respectively. These distributions are compared with those of the experimental data [26], denoted by the dotted symbols. It is clear that the long-dashed distributions are in poor agreement with the experimental data, especially for small r. Considering the higher orbitals $2s_{1/2}$ and $1f_{7/2}$ due to introducing the parameters α_1 and α_2 into the calculations leads to a good agreement with the experimental data as shown by the solid curves.

The dependence of $n(k)$ (in fm^3) on k (in fm^{-1}) for ^{6}Li, ^{10}B, ^{12}C and ^{14}N nuclei are shown in figure 2. The dash–dotted curves represent the calculated NMD of eq. (9)

Table 1. Parameters of the NDD of 1p-shell nuclei

Nucleus	Parameters of the experimental NDD [26]				$\rho_{exp}(0)$ (fm^{-3}) [26]	$\langle r^2\rangle_{exp}^{1/2}$ (fm) [26]	b (fm)	α	α_1	α_2	Q
	Model	c or a (fm)	z or t (fm)	w							
^{6}Li	2PF	1.447	0.61		0.154	2.5	1.7	1.059	0.143	0.916	
^{10}B	HO	1.63	0.837		0.1831	2.442	1.63	0.861	0.278	0.583	1.6
^{12}C	2PF	2.24	0.5		0.1688	2.476	1.65	0.585	0.149	0.435	
^{14}N	3PF	2.57	0.515	−0.19	0.1792	2.55	1.68	0.871	0.489	0.382	18.8

The values are given for the parameters c and z if the 2PF or 3PF model is used, for the parameters a and t if the HO model is used and the parameter w if the 3PF model is used.

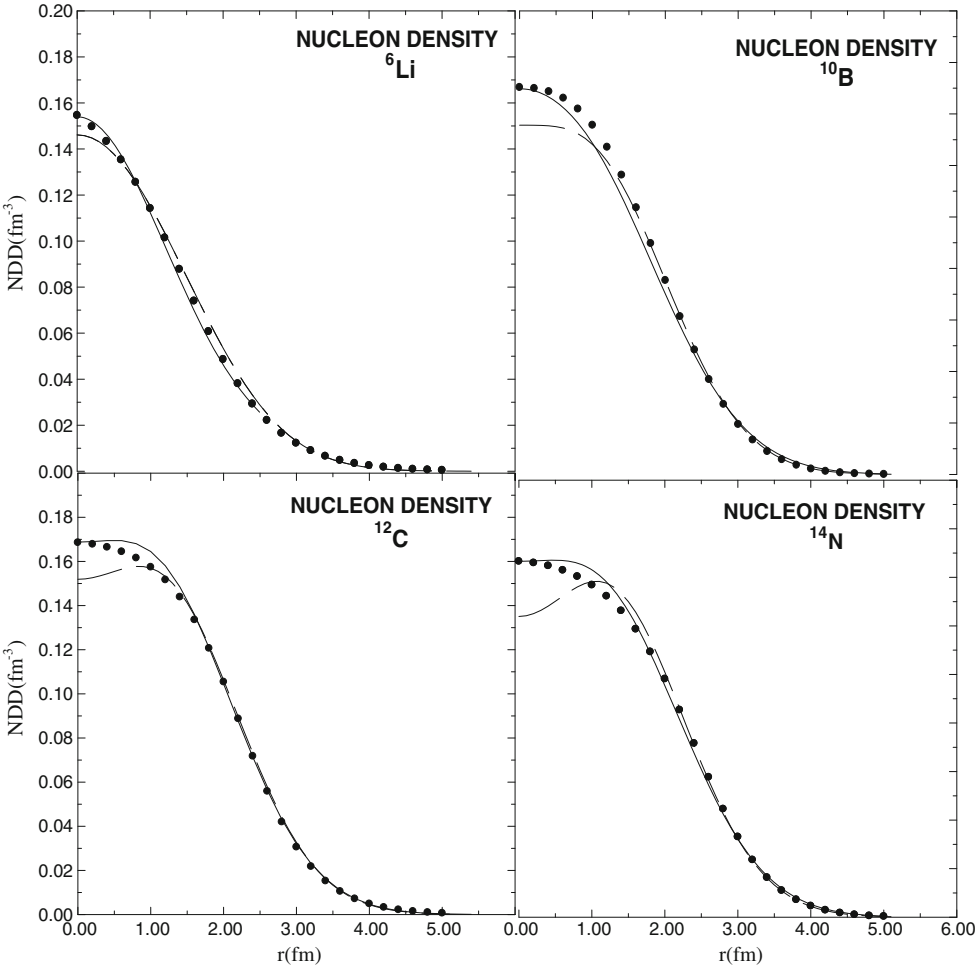

Figure 1. Dependence of NDD on r for ^{6}Li, ^{10}B, ^{12}C and ^{14}N nuclei. The long-dashed and solid curves are the calculated NDD of eq. (2) when $\alpha = \alpha_1 = \alpha_2 = 0$ and $\alpha \neq \alpha_1 \neq \alpha_2 \neq 0$, respectively. The dotted symbols are the experimental data of ref. [26].

obtained by the shell model calculation using the single-particle harmonic oscillator wave functions in momentum representation. The dotted symbols and solid curves are the NMD obtained by the CDFM of eq. (21) using the experimental and theoretical NDD, respectively. It is obvious that the behaviour of the distributions obtained by the shell model calculations are in contrast with the distributions reproduced by the CDFM. The main feature of the distributions represented by the dash–dotted curve is the steep slope behaviour when k increases. This behaviour is in disagreement with other studies [18,21–23] and it is attributed to the fact that the ground state shell model wave function given in terms of a Slater determinant does not take into account the important effect of the short-range dynamical correlation functions. Hence, the short-range repulsive features

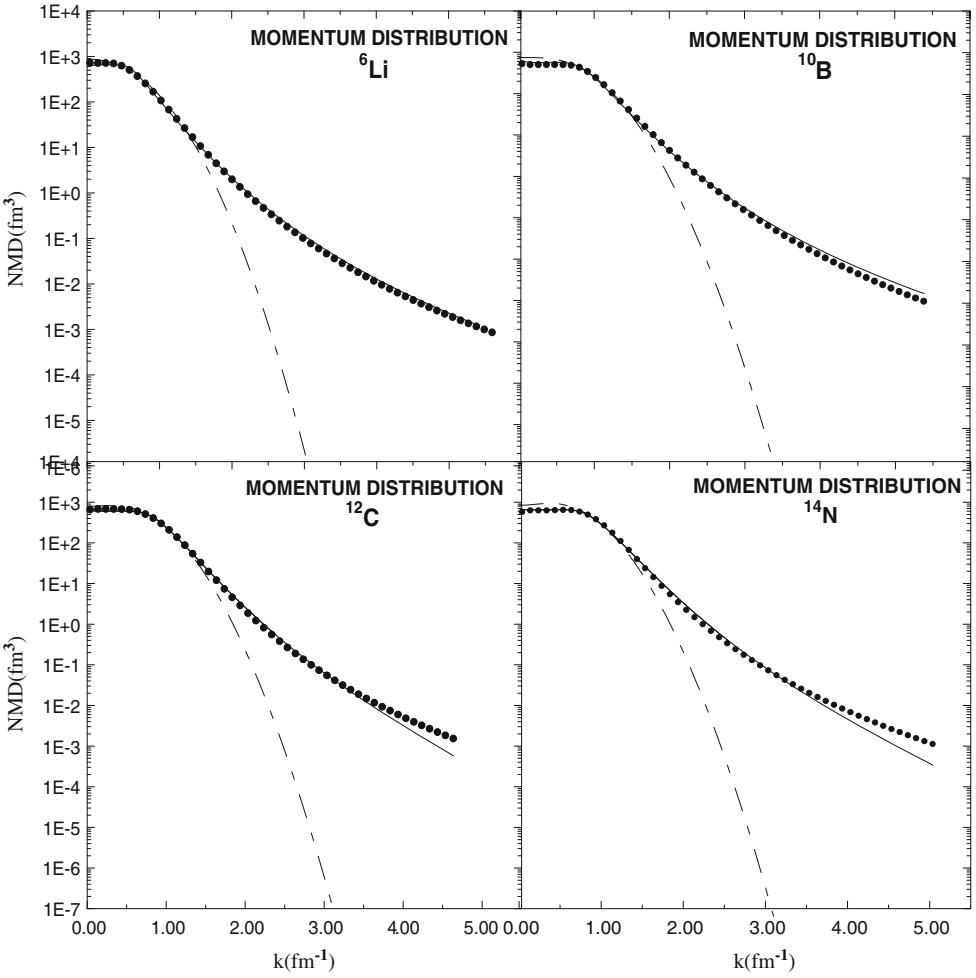

Figure 2. Dependence of NMD on k for ^{6}Li, ^{10}B, ^{12}C and ^{14}N nuclei. The solid curves and dotted symbols are the calculated NMD obtained in terms of the CDFM of eq. (21) using the theoretical NDD of eq. (2) and the experimental data [26], respectively. The dash–dotted curves are the calculated NMD of eq. (9) obtained by the shell model calculations using the single-particle harmonic oscillator wave functions in momentum representation.

of the nucleon–nucleon forces are responsible for the high-momentum behaviour of the NMD [21,22]. It is seen that the general structure of the dotted and solid distributions at the region of high-momentum components is almost the same for ^{6}Li, ^{10}B, ^{12}C and ^{14}N nuclei, where these distributions have the feature of long-tail behaviour at momentum region $k \geq 2$ fm^{-1}. The feature of the long-tail behaviour obtained by the CDFM is related to the existence of high densities $\rho_x(r)$ in the decomposition of eq. (15), though their weight functions $|f(x)|^2$ are small.

The dependence of $F(q)$ on q (in fm^{-1}) for ^{6}Li and ^{12}C nuclei is shown in figure 3. The solid curves are the calculated $F(q)$s obtained by the framework of CDFM using the theoretical weight function of eq. (27). The symbols, in this figure, represent the experimental data. In ^{6}Li nucleus, the calculated form factors are in very good agreement with the experimental data of ref. [10] (open circles) and ref. [33] (triangles) throughout all values of momentum transfer q. In the ^{12}C nucleus, the calculated form factors agree quite well with those of experimental data of ref. [34] (open circles), ref. [35] (rhombs) and ref. [36] (triangles) up to momentum transfer $q \approx 1.85$ fm^{-1} and underestimate these data when $q > 1.85$ fm^{-1}. It is evident from this figure that the calculated results of ^{12}C predicate the location of the observed first diffraction minimum very well.

The dependence of $F(q)$ on q (in fm^{-1}) for ^{10}B and ^{14}N nuclei is shown in figure 4. The dashed and dash–dotted curves represent the contributions of the monopole form factors $F_{C0}(q)$ and quadrupole form factors $F_{C2}(q)$, respectively, while the solid curves represent the total contribution $F(q)$, which is the sum of $F_{C0}(q)$ and $F_{C2}(q)$. Here, the experimental data are represented by the symbols. In ^{10}B nucleus, the calculated $F_{C0}(q)$ is not able to give a satisfactory description of the experimental data of ref. [37] (open circles) and ref. [32] (triangles) for the region of momentum transfer $q > 1.4$, but once the contribution of $F_{C2}(q)$ is added to $F_{C0}(q)$, the obtained $F(q)$ will be in excellent agreement with the experimental data as shown by the solid curve. In ^{14}N nucleus, the experimental data of ref. [38] (open circles) are very well described by the calculated $F_{C0}(q)$ up to momentum transfer $q \approx 1.6$ fm^{-1}, whereas for $q > 1.6$ fm^{-1} the calculated $F_{C0}(q)$ underestimate these experimental data. It is very clear that the contribution of $F_{C2}(q)$ gives a strong modification to $F_{C0}(q)$ and bring the calculated values very close

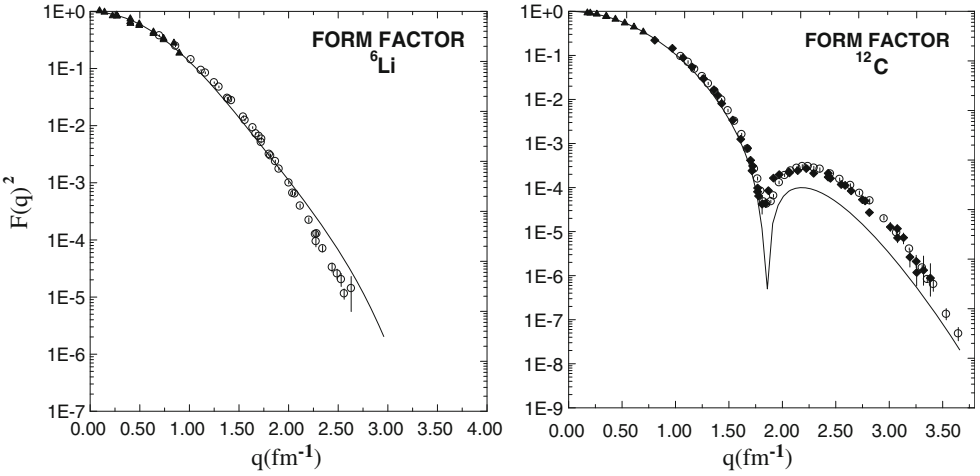

Figure 3. Dependence of the form factors on q for ^{6}Li and ^{12}C nuclei. The solid curves are the form factors calculated using eq. (23). The experimental data for ^{6}Li are taken from ref. [10] (open circles) and ref. [33] (triangles) while the experimental data for ^{12}C are taken from ref. [34] (open circles), ref. [35] (rhombs) and ref. [36] (triangles).

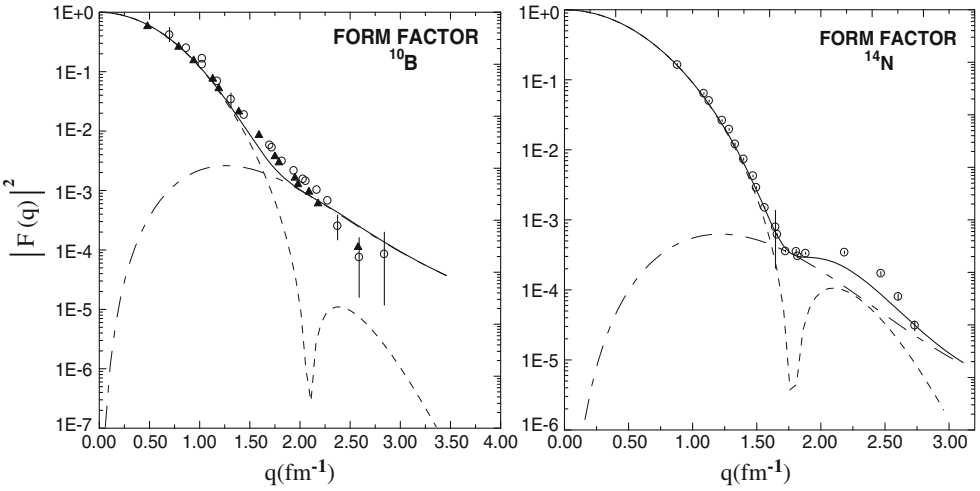

Figure 4. Dependence of the form factors on q for ^{10}B and ^{14}N nuclei. The dashed and dash–dotted curves represent the contribution of the monopole form factors $|F_{C0}(q)|^2$ and the quadrupole form factors $|F_{C2}(q)|^2$, respectively. The solid curves represent the form factors of both contributions. The experimental data for ^{10}B are taken from ref. [37] (open circles) and ref. [32] (triangles) while the experimental data for ^{14}N are taken from ref. [38] (open circles).

to the experimental data. Besides, the location of the first diffraction minimum is located in the correct place when the contribution of $F_{C2}(q)$ is included in the calculations.

4. Summary and conclusions

The NMD and elastic electron scattering form factors calculated using CDFM are expressed in terms of the weight function $|f(x)|^2$. The weight function, which is related to the local density $\rho(r)$, is obtained from the theory and the experiment. The feature of the long-tail behaviour of the NMD is reproduced by both the theoretical and experimental weight functions and is related to the existence of high densities $\rho_x(r)$ in the decomposition of eq. (15), though their weight functions are small. The experimental form factors for elastic electron scattering from ^{6}Li and ^{12}C nuclei are well reproduced by the monopole form factors. It is found that the contribution of the quadrupole form factors in ^{10}B and ^{14}N nuclei, which are described by the undeformed p-shell model, are essential to obtain a remarkable agreement between the theoretical and experimental form factors. It is concluded that the derived form of NDD of eq. (2) employed in the determination of theoretical weight function of eq. (27) is capable to reproduce information about the NMD and elastic form factors as do those of the experimental data.

References

[1] T W Donnelly and I Sick, *Rev. Mod. Phys.* **56**, 461 (1984)

[2] I Sick, *Prog. Part. Nucl. Phys.* **47**, 245 (2001)
[3] R Hofstadter, B Hahn, A W Knudsen and J A Mclntyre, *Phys. Rev.* **95**, 512 (1954)
[4] R Hofstadter, *Rev. Mod. Phys.* **28**, 214 (1956)
[5] G Fricke, C Bernhardt, K Heiling, L A Schaller, L Shellenberg, E B Shera and C W de Jager, *At. Data Nucl. Data Tables* **60**, 177 (1995)
[6] I Angeli, *At. Data Nucl. Data Tables* **87**, 185 (2004)
[7] X Roca-Maza, M Centelles, F Salvat and X Vinas, *Phys. Rev.* **C78**, 044332 (2008)
[8] J D Walecka, *Electron scattering for nuclear and nucleon structures* (Cambridge University Press, United Kingdom, 2004)
[9] Y Chu, Z Ren, T Dong and Z W Wang, *Phys. Rev.* **C79**, 044313 (2009)
[10] L R Suelzle, M R Yearian and Hall Crannell, *Phys. Rev.* **162**, 992 (1967)
[11] R Anni, G Có and P Pellegrino, *Nucl. Phys.* **A584**, 35 (1995)
[12] R A Radhi, A A Abdullah, Z A Dakhil and N M Adeeb, *Nucl. Phys.* **A696**, 442 (2001)
[13] R B Wiringa and R Schiavilla, *Phys. Rev. Lett.* **81**, 4317 (1998)
[14] E Cravo, *Phys. Rev.* **C54**, 523 (1996)
[15] Z Wang and Z Ren, *Phys. Rev.* **C71**, 054323 (2005)
[16] R A Radhi, *Nucl. Phys.* **A71**, 100 (2003)
[17] A N Antonov, D N Kadrev, M K Gaidarov, E Moya de Guerra, P Sarriguren, J M Udias, V K Lukyanov, E V Zemlyanaya and G Z Krumova, *Phys. Rev.* **C72**, 044307 (2005)
[18] A N Antonov, P E Hodgson and I Zh Petkov, *Nucleon momentum and density distribution in nuclei* (Clarendon Press, Oxford, 1988)
[19] S Frankel, W Frati, O Van Dyck, R Werbeck and V Highland, *Phys. Rev. Lett.* **36**, 642 (1976)
[20] V I Komarov, G E Kosarev, H Muler, D Netzband and T Stiehler, *Phys. Lett.* **B69**, 37 (1977)
[21] Ch C Moustakidis and S E Massen, *Phys. Rev.* **C62**, 034318 (2000)
[22] M Traini and G Orlandini, *Z. Phys.* **A321**, 479 (1985)
[23] M Dal Ri, S Stringarl and O Bohigas, *Nucl. Phys.* **A376**, 81 (1982)
[24] A N Antonov, V A Nikolaev and I Zh Petkov, *Z. Phys.* **A297**, 257 (1980)
[25] A N Antonov, P E Hodgson and I Zh Petkov, *Nucleon correlation in nuclei* (Springer-Verlag, Berlin–Heidelberg–New York, 1993)
[26] H De Vries, C W De Jager and C De Vries, *At. Data Nucl. Data Tables* **36**, 495 (1987)
[27] W Reuter, G Fricke, K Merle and H Miska, *Phys. Rev.* **C26**, 806 (1982)
[28] K N Flaih, *Calculations of longitudinal electron scattering form factors for the 2s–1d shell nuclei using ground state charge density distribution*, Ph.D. thesis (College of Science, University of Baghdad, 2007)
[29] K S Jassim, *Nucleon–nucleon realistic interactions in electron scattering with core polarization*, Ph.D. thesis (College of Science, University of Baghdad, 2007)
[30] A R Ridha, *Elastic electron scattering form factor and nuclear momentum distributions in enclosed and open shell nuclei*, M.Sc. thesis (University of Baghdad, 2006)
[31] B A Brown, R A Radhi and B H Wildenthal, *Phys. Rep.* **101**, 313 (1983)
[32] T Stovall, J Goldemberg and D B Isabelle, *Nucl. Phys.* **86**, 225 (1966)
[33] F A Bumiller, F R Buskirk, J N Dyer and W A Monson, *Phys. Rev.* **C5**, 391 (1972)
[34] I Sick and J S McCarthy, *Nucl. Phys.* **A150**, 631 (1970)
[35] H Crannell, *Phys. Rev.* **148**, 1107 (1966)
[36] J A Jansen, R Th Peerdeman and C De Vries, *Nucl. Phys.* **A188**, 337 (1972)
[37] A Cichocki, J Dubach, R S Hicks, G A Peterson, C W de Jager, H de Vries, N Kalantar-Nayestanaki and T Sato, *Phys. Rev.* **C51**, 2406 (1995)
[38] E B Dally, M G Croissiaux and B Schweitz, *Phys. Rev.* **C2**, 2057 (1970)